Thermal Behavior of β-1 Subunits in Lignin: Pyrolysis of 1,2-Diarylpropane-1,3-diol-type Lignin Model Compounds

ARTICLE *in* JOURNAL OF AGRICULTURAL AND FOOD CHEMISTRY · MAY 2007

Impact Factor: 2.91 · DOI: 10.1021/jf0628126 · Source: PubMed

4 AUTHORS, INCLUDING:

Tatsuya Ashitani
Yamagata University
37 PUBLICATIONS **197** CITATIONS
SEE PROFILE

Koki Fujita
Kyushu University
29 PUBLICATIONS **327** CITATIONS
SEE PROFILE

JOURNAL OF AGRICULTURAL AND FOOD CHEMISTRY

Thermal Behavior of β-1 Subunits in Lignin: Pyrolysis of 1,2-Diarylpropane-1,3-diol-type Lignin Model Compounds

KEN-ICHI KURODA,*,† TATSUYA ASHITANI,† KOKI FUJITA,† AND TAKEFUMI HATTORI‡

Department of Forest and Forest Products Sciences, Faculty of Agriculture, Kyushu University, 6-10-1 Hakozaki, Higashi-ku, Fukuoka 812-8581, Japan, and Research Institute for Sustainable Humanosphere, Kyoto University, Uji 611-0011, Japan

1,2-Diarylpropane-1,3-diol-type lignin model compounds, 1,2-bis(4-hydroxy-3-methoxyphenyl)propane-1,3-diol (**1**) and 1-(3,4-diethoxyphenyl)-2-(4-methoxyphenyl)propane-1,3-diol (**2**), were pyrolyzed at 500 °C for 4 s to clarify the thermal behavior of β-1 subunits in lignin. Products were monitored by gas chromatography/mass spectrometry. The cleavage of the Cα−Cβ bond to produce benzaldehydes such as 4-hydroxy-3-methoxybenzaldehyde (**9**) and phenylethanals as the counterparts such as 4-hydroxy-3-methoxyphenylethanal (**10**) occurred in pyrolyses of both **1** and **2**. In pyrolysis of **1**, an oxetane pathway leading to the formation of *Z*/*E*-stilbenes without the γ-CH_2OH group such as *Z*/*E*-4,4′-dihydroxy-3,3′-dimethoxystilbene (**3**) was predominant. In pyrolysis of **2**, the oxetane pathway was minor, while pathways producing a dimer with a =CγH_2 group by loss of water and a dimer with an α-carbonyl group were predominant. Pyrolysis of Japanese cedar wood provided **3** and **10** in ∼0.8% and 0.6% yields, respectively, based on the Klason lignin content, while pyrolysis of a guaiacyl bulk dehydrogenation polymer gave them in a very small amount.

KEYWORDS: Lignin; β-1 subunits; oxetane; stilbene; pyrolysis−gas chromatography/mass spectrometry; Japanese cedar wood; guaiacyl dehydrogenation polymer

INTRODUCTION

Lignin forms an integral part of all vascular plants, providing them mechanical support to life on land, defense, and water transport systems. Although it, next to cellulose, is abundantly present [15−36% of woody plants (*1*)], the main use is as an energy source. To utilize lignin and lignin-containing materials effectively, a better understanding of the lignin structure is required. However, polymer complexities of lignin, such as a randomly cross-linked three-dimensional system connected by irregular C−C and C−O−C linkages and close association with other cell wall polymers, make lignin analysis difficult. Such a situation encountered in lignin chemistry has opened up the possibility of developing new analytical procedures as alternatives to chemical and spectroscopic techniques traditionally employed in the field of lignin chemistry.

Pyrolysis combined with gas chromatography (GC) or GC/mass spectrometry (MS) has shown usefulness as a powerful analytical technique in the field of lignin chemistry (*2*) because of sensitivity, less sample preparation steps, and short analysis time. Under controlled pyrolysis conditions, lignin polymers are reproducibly broken to produce diagnostic monomeric and oligomeric phenols, which should preserve the structural attributes of the main subunits in lignin. However, the relationships between subunits and products remain unclear and are still controversial. This inherent problem associated with pyrolysis procedures restricts further applications of pyrolysis−GC and −GC/MS procedures to lignin analysis. To resolve this limitation, clarification of the thermal behavior of each lignin subunit is required, because lignin comprises diverse subunits.

This paper addresses the thermal behavior of β-1 subunit, which is shown as one of the major subunits in lignin by mild hydrolysis (*3*) and thioacidolysis (*4*). Recent studies show that β-1 subunits are actually present as spirodienone structures with roughly 3−4% abundance in lignin (*5*−*7*), which produce traditional β-1 subunits upon chemical treatments such as acidolysis; this might be true for pyrolysis. Although the abundance of traditional β-1 subunits varies 1−15% in spruce lignin (*8*−*10*), depending on analytical methods employed, pyrolysis products derived from β-1 subunits often have been reported (*11*−*13*). However, a few data on the thermal behavior of β-1 subunits are available (*12*). In this study, to simplify the interpretation of the thermal behavior of β-1 subunits in lignin, we used two 1,2-diarylpropane-1,3-diol (β-1) lignin model compounds, 1,2-bis(4-hydroxy-3-methoxyphenyl)propane-1,3-diol (**1**) and 1-(3,4-diethoxyphenyl)-2-(4-methoxyphenyl)propane-1,3-diol (**2**) (see **Figure 1** for their structures). Pyrolysis products were monitored by GC/MS and compared with those of softwood synthetic and native lignins.

* Corresponding author: phone +81 92 642 2988; e-mail kenfumi@agr.kyushu-u.ac.jp.
† Kyushu University.
‡ Kyoto University.

10.1021/jf0628126 CCC: $37.00
Published on Web 03/27/2007

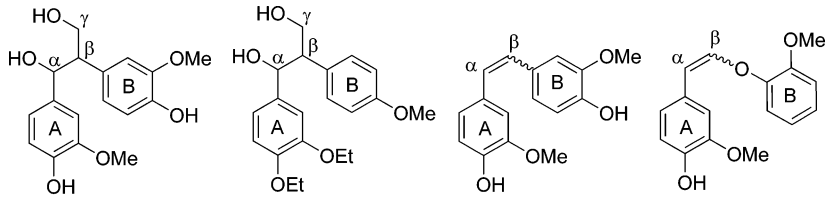

Figure 1. Authentic dimers **1**–**4**.

Table 1. Pyrolysis Products of **1**

peak	product[a]	partial mass spectrum, *m*/*z* (rel int, %)	rel contribution (%)
5	2-methoxyphenol	124 (M^+, 72), 109 (100), 81 (71), 53 (46)	16.3
6	2-methoxy-4-methylphenol	138 (M^+, 94), 123 (100), 95 (33), 77 (23), 67 (31)	4.2
7	4-ethyl-2-methoxyphenol	152 (M^+, 50), 137 (100), 77 (22)	0.5
8	4-hydroxy-3-methoxystyrene	150 (M^+, 100), 135 (91), 107 (39), 77 (48)	0.8
9	4-hydroxy-3-methoxybenzaldehyde	152 (M^+, 87), 151 (100), 123 (21), 109 (22), 81 (36)	7.6
10	4-hydroxy-3-methoxyphenylethanal	166 (M^+, 23), 137 (100), 122 (23)	8.0
11	unknown	180 (M^+, 15), 151 (100), 119 (31), 91 (58)	2.2
12	unknown	178 (M^+, 67), 150 (25), 149 (100), 117 (21), 89 (42), 78 (26), 77 (35)	1.7
Z-**3**	*Z*-4,4′-dihydroxy-3,3′-dimethoxystilbene	273 (21), 272 (M^+, 100), 211 (18), 207 (12), 137 (17), 57 (55).	9.6
Z-**13**	*Z*-4-[2-(4-hydroxy-3-methoxyphenyl)prop-1-enyl]-2-methoxyphenol	287 (17), 286 (M^+, 100), 272 (4), 271 (5), 225 (14), 211 (12), 162 (13), 128 (17), 115 (17), 91 (21), 76 (21)	2.6
14	4-[2-(4-hydroxy-3-methoxyphenyl)ethyl]-2-methoxyphenol	274 (M^+, 5), 137 (100), 122 (10)	6.8
E-**3**	*E*-form of **3**	273 (17), 272 (M^+, 100), 211 (19), 106 (11), 84 (16), 76 (13)	34.8
E-**13**	*E*-form of **13**	287 (19), 286 (M^+, 100), 272 (14), 271 (41), 211 (16), 165 (17), 153 (12), 152 (16)	4.7
	total		99.8

[a] Product structures refer to those in **Figures 1** and **3** and **Scheme 1**.

MATERIALS AND METHODS

Melting points were uncorrected. ^{1}H nuclear magnetic resonance (NMR) spectra were obtained on a Bruker 500 or JEOL AL400 spectrometer with deuterium chloroform and were reported by chemical shifts (relative to tetramethylsilane), splitting patterns, integration areas, and proton assignments. Electron ionization mass spectrometry (EI-MS) analysis employed a Shimadzu GC/MS, model QP 5000, a DB-5 fused-silica capillary column (GL Science, 30 m × 0.25 mm, film thickness 0.25 μm) with a column temperature program of 50 (1 min) to 320 °C (12 min hold) ramped at 5 °C min^{-1} or a Quadrex MS fused-silica capillary column (Quadrex, 25 m × 0.25 mm, film thickness 0.25 μm) with a column temperature program of 50 (1 min) to 280 °C (13 min hold) ramped at 5 °C min^{-1}, carrier gas helium (flow rate 1.3 mL min^{-1}), injection and detector ports heated at 280 °C, a 1:100 split ratio, 70 eV ionization voltage in a 200 °C ion chamber, mass range *m*/*z* 50−600. Data were collected by Shimadzu LabSolution software (version 1.02). Product assignments were carried out by searching a NIST 62 database, by comparing MS data with published data (*2*, *14*), and by interpreting MS data.

Materials. Diol **1** was prepared according to the method of Ahvonen et al. (*15*): mp 155−156 °C [lit. (*15*) 151−154 °C]. Structure confirmation was provided by NMR and EI-MS; the numbering systems of side chains α, β, and γ and rings A and B are provided in **Figure 1**. NMR (tetraacetate, $CDCl_3$) δ_H 1.98 (6H, s, 2 × alcoholic-OAc), 2.27 (3H, s, Ar−OAc), 2.29 (3H, s, Ar−OAc), 3.38 (1H, dd, J = 13.4, 6.7 Hz, β-H), 3.70 (3H, s, Ar−OCH_3), 3.73 (3H, s, Ar−OCH_3), 4.18 (1H, dd, J = 11.3, 7.1 Hz, γ-Ha), 4.39 (1H, dd, J = 11.3, 7.1 Hz, γ-Hb), 6.10 (1H, d, J = 6.5 Hz, α-H), 6.61 (2H, dd, J = 13.5, 1.9 Hz, Ar−H), 6.77 (1H, dd, J = 8.2, 1.9 Hz, Ar−H), 6.82 (1H, dd, J = 8.2, 1.9 Hz, Ar−H), 6.96 (2H, d, J = 8.1 Hz, Ar−H); EI-MS (tetraacetate) *m*/*z* (%) 488 (M^+, <1), 446 (M − 42, 35), 237 (10), 209 (17), 195 (44), 192 (18), 153 (64), 150 (100).

Diol **2**: mp 83.5−84.8 °C; NMR (diacetate, $CDCl_3$) δ_H 1.39 (3H, t, J = 7.1 Hz, Ar−OCH_2CH_3), 1.44 (3H, t, J = 7.1 Hz, Ar−OCH_2CH_3), 1.94 (3H, s, alcoholic-OAc), 1.96 (3H, s, alcoholic-OAc), 3.33 (1H, q, J = 6.8 Hz, β-H), 3.79 (3H, s, Ar−OCH_3), 4.00 (2H, q, J = 7.0 Hz, Ar−OCH_2CH_3), 4.03−4.11 (3H, m, Ar−OCH_2CH_3 + γ-Ha), 4.26 (1H, q, J = 6.6 Hz, γ-Hb), 6.01 (1H, d, J = 7.6 Hz, α-H), 6.62 (1H, d, J = 1.7 Hz, Ar−H), 6.80 (4H, m, Ar−H), 7.07 (1H, d, J = 1.9 Hz, Ar−H), 7.09 (1H, d, J = 1.9 Hz, Ar−H); EI-MS (diacetate) *m*/*z* (%) 430 (M^+, 4), 237 (24), 195 (100), 134 (16).

1,2-Bis(4-hydroxy-3-methoxyphenyl)ethene (**3**), 4,4′-dihydroxy-3,3′-dimethoxystilbene, was prepared by decarboxylation and deacetylation of 2,3-bis(4-acetoxy-3-methoxyphenyl)acrylic acid according to the method of Gierer et al. (*16*): mp 217−218 °C [lit. (*16*) 215−216 °C]; NMR (diacetate, $CDCl_3$) δ_H 2.33 (6H, s, 2 × Ar−OAc), 3.90 (6H, s, Ar−OCH_3), 7.01−7.10 (8H, m, Ar-6H + olefinic-2H); EI-MS (diacetate) *m*/*z* (%) 356 (M^+, 11), 314 (M − 42, 19), 272 [M − (2 × 42), 100]. Stilbene **3** consisted of 97% *E*-form and 3% *Z*-form on the basis of the GC peak areas.

1-(4-Hydroxy-3-methoxyphenyl)-2-(2-methoxyphenoxy)ethene (**4**) consisting of *Z*- and *E*-isomers with a roughly 2:1 GC signal area ratio was synthesized by treating 4-[1-hydroxy-2-(2-methoxyphenoxy)ethyl]-2-methoxyphenol with bromotrimethylsilane and then 1,8-diazobicyclo-[5.4.0]undec-7-ene (*17*): EI-MS *m*/*z* (%) 272 (M^+, 100), 211 (59), 137 (55), 133 (43), 77 (55). It was prepared when required because of its instability under neutral and acidic conditions (*18*).

As reference lignins, Japanese cedar (*Cryptomeria japonica* D. Don) wood and a bulk guaiacyl dehydrogenation polymer (DHP) were employed, which were the same as those employed previously (*19*, *20*). The cedar wood was ground in a Wiley mill, and meals less than 60 mesh were Soxhlet-extracted with ethanol−benzene (1/2 v/v) for 6 h. After air-drying, the extractive-free cedar wood meals were subjected to pyrolysis−GC/MS and pyrolysis−GC analyses.

Pyrolysis−GC/MS. The pyrolysis−GC/MS system was a combination of a JHP-5 model Curie-point pyrolyzer (Japan Analytical Industry, Tokyo, Japan) and a model QP5000 GC/MS (Shimadzu, Kyoto, Japan). Basically, this system is similar to that with a JHP-3 pyrolyzer (Japan Analytical Industry) and an HP 5890 series II gas chromatograph (Hewlett-Packard, Palo Alto, CA) with an HP 5972A quadrupole mass selective detector (Hewlett-Packard) employed previously (*21*). The sample (~20 μg for the model compounds, ~50−70 μg for the DHP, and ~100−200 μg for the cedar wood) was tightly wrapped with a ferromagnetic alloy made of 40% iron and 60% nickel (pyrofoil), and

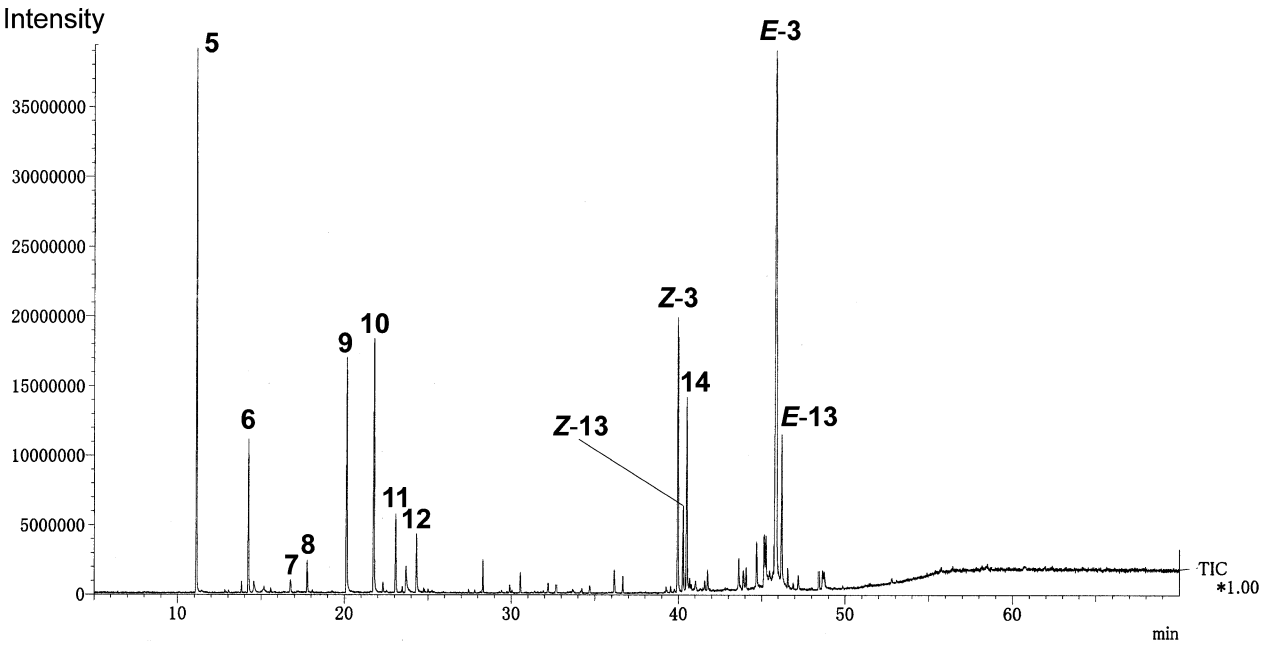

Figure 2. Pyrolysis–GC/MS trace of **1**. Pyrolysis was carried out at 500 °C for 4 s. Product names refer to those in **Table 1**; structures are given in **Figures 1** and **3** and **Scheme 1**.

Table 2. Pyrolysis Products of **2**

peak	product[a]	partial mass spectrum, *m*/*z* (rel int, %)	rel contribution (%)
15	methoxybenzene	108 (M^+, 100), 78 (85), 65 (91), 51 (37)	0.2
16	4-methoxy-1-methylbenzene	122 (M^+, 100), 121 (54), 107 (33), 91 (31), 79 (34), 77 (66), 63 (24)	1.1
17	4-methoxystyrene	134 (M^+, 100), 119 (59), 91 (61), 65 (50), 63 (24)	1.8
18	1,2-diethoxybenzene	166 (M^+, 20), 110 (100), 109 (28)	1.8
19	4-methoxyphenylethanal	150 (M^+, 13), 121 (100)	9.2
20	3,4-diethoxybenzaldehyde	194 (M^+, 29), 138 (62), 137 (100), 109 (17), 81 (20)	17.7
Z-**21**	*Z*-3,4-diethoxy-4′-methoxystilbene	299 (25), 298 (M^+, 100), 213 (26), 195 (47), 181 (40), 169 (18), 165 (22), 153 (31), 152 (59), 141 (24), 139 (15), 121 (18), 115 (36)	1.9
22	1-(3,4-diethoxyphenyl)-2-(4-methoxyphenyl) ethan-1-one	314 (M^+, 3), 193 (100), 165 (32), 137 (31), 121 (26), 109 (14)	26.0
E-**21**	*E*-form of **21**	see **Scheme 2** and **Figure 5**	4.3
23	1-(3,4-diethoxyphenyl)-2-(4-methoxyphenyl) prop-2-en-1-one	326 (M^+, 28), 297 (10), 281 (14), 269 (10), 194 (16), 193 (100), 179 (24), 165 (60), 151 (17), 137 (85), 135 (30), 133 (74), 118 (20), 109 (38)	2.4
24	1-(3,4-diethoxyphenyl)-2-(4-methoxyphenyl) prop-2-en-1-ol	328 (M^+, <1), 195 (12), 194 (10), 134 (100), 111 (11), 93 (20)	33.6
	total		100

[a] Product structures refer to those in **Figures 1** and **3** and **Scheme 1**.

the sample-loaded pyrofoil was inserted in the top of the sample tube in the pyrolyzer heated at 250 °C; the pyrolyzer has a permanent magnet located close to the sample tube. The magnet located outside the top of the tube held the pyrofoil until the GC/MS conditions had been settled. Pyrolysis at 500 °C for 4 s under helium atmosphere was triggered as soon as the foil released by the magnet fell to the bottom. Products were sent to the GC/MS via a transfer line heated at 250 °C. Products of the model compounds and reference lignins were separated on the DB-5 and Quadrex MS fused-silica capillary columns, respectively; therefore, absolute retention times slightly differed between model compound and reference lignin runs. Triplicate analyses were performed for each sample.

Pyrolysis−GC. The pyrolysis−GC system was the same as that employed previously (*22*, *23*). Briefly, it was a combination of a Curie-point pyrolyzer (JHP-3 model, Japan Analytical Industry) heated at 250 °C and a Shimadzu GC-17A gas chromatograph (Kyoto, Japan) with a flame ionization detector (FID). The cedar wood meals (∼100−200 μg) and the DHP (∼50−70 μg) were pyrolyzed at 500 °C for 4 s in the pyrolyzer heated at 250 °C. The volatile products were sent, via a transfer line at heated at 250 °C, to the GC with a Quadrex MS fused-silica capillary column (Quadrex, 25 m × 0.25 mm, film thickness 0.25 μm). The column temperature program was the same as that employed in the pyrolysis−GC/MS with the same column. The injection with a 1:100 split ratio and FID ports were kept at 280 °C. Helium as the carrier gas (flow rate = 1.3 mL min^{-1}) was employed. Duplicate analyses were performed for each sample.

RESULTS AND DISCUSSION

Lignin model compounds are often employed to simplify the study of the thermal behavior of corresponding lignin subunits because of the difficulty associated with the characterization of structural changes of lignin due to large thermal energy. In this study, diols **1** and **2** were selected to represent phenolic and nonphenolic β-1 subunits in lignin, respectively. The use of **2** with different rings A and B helped in clarification of pyrolytic sources for monomeric products.

Pyrolysis−GC/MS of 1. Figure 2 shows the pyrolysis−GC/MS trace of **1**. **Table 1** lists identified products with the relative contributions (%) and partial mass data; products **11** and **12** with each ∼2% contribution were unknown. Relative contributions were determined by normalizing GC/MS signal areas of identified products at 100%.

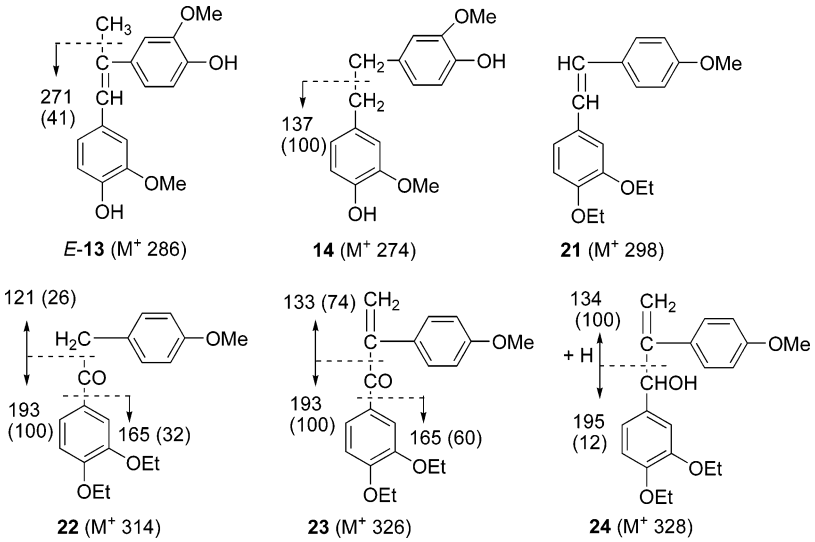

Figure 3. Identified dimers and their proposed mass fragmentations [*m*/*z* (%)]. Product names refer to those in **Tables 1** and **2**.

Scheme 1. Selected Pyrolytic Pathways of **1** and **2**[a]

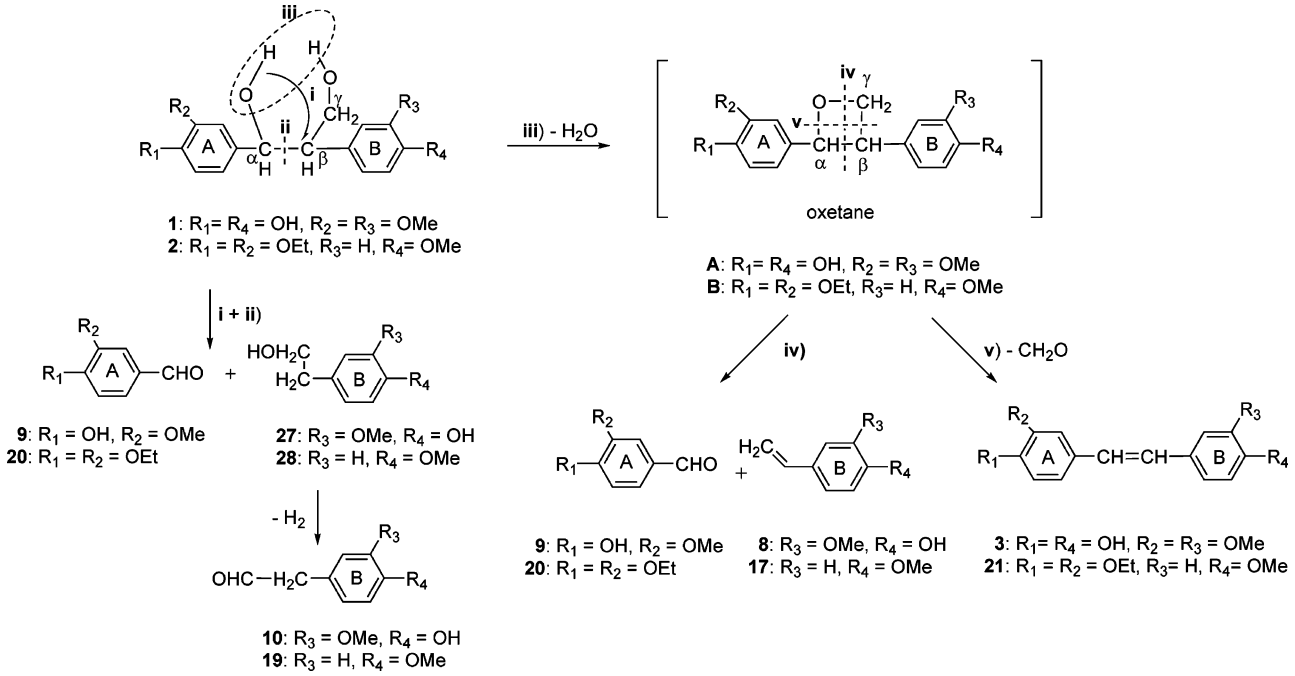

[a] Product names refer to those in **Tables 1** and **2.**

Monomeric products **5**−**12** appeared below 30 min retention time. On the basis of the library search, the earliest eluting product was ascribed to 2-methoxyphenol (**5**), which is produced by the cleavage of either the bond between ring A and the Cα atom or the bond between ring B and the Cβ atom. The formation of **5** is noted, because so far we observed no production of **5** in such a large contribution (relative contribution 16.3%) in pyrolysis of β-5 (*19*), β-β (*20*), β-aryl ether (*24*), and coniferyl alcohol end groups (*25*) type lignin dimeric model compounds, in spite of **5** being a main pyrolysis product of lignin. 2-Methoxy-4-methylphenol (**6,** ∼4%) may stem from moiety B [see the following discussion on the production of 4-methoxy-1-methylbenzene (**16**) in pyrolysis of **2**].

A 7.6% contribution was given by **9** attributed to 4-hydroxy-3-methoxybenzaldehyde. Since **9** is produced by cleavage of the Cα−Cβ bond, the contribution of its counterpart stemming from moiety B should equal that of **9**. It is rationalized that 4-hydroxy-3-methoxyphenylethanal (**10**) with an 8% contribution is the counterpart of **9**.

These findings suggest that **5**, **6**, **9**, and **10** produced in pyrolysis of softwood lignin partly stem from β-1 subunits. To our knowledge, this is a first report showing that the β-1 subunit is a source for **10** in pyrolysis of softwood lignin.

The formation of β-aldehyde **10** is explainable by considering the formation of 4-hydroxy-3-methoxyphenylethanol (**27**) not detected in this study. Hydrogen migration from the α-OH group onto the Cβ atom of **1** (pathway i in **Scheme 1**) and successive cleavage of the Cα−Cβ bond (pathway ii) give a pair of **9** and **27**. Removal of a hydrogen molecule from the β-CH_2OH group of **27** provides β-aldehyde **10**.

α-Aldehyde **9** is produced also from an oxetane intermediate (oxetane A) (*26*), which is provided by α,γ-dehydration between the OH group at the α-position and the proton of the Cγ-OH (pathway iii). Unstable oxetane A is immediately decomposed

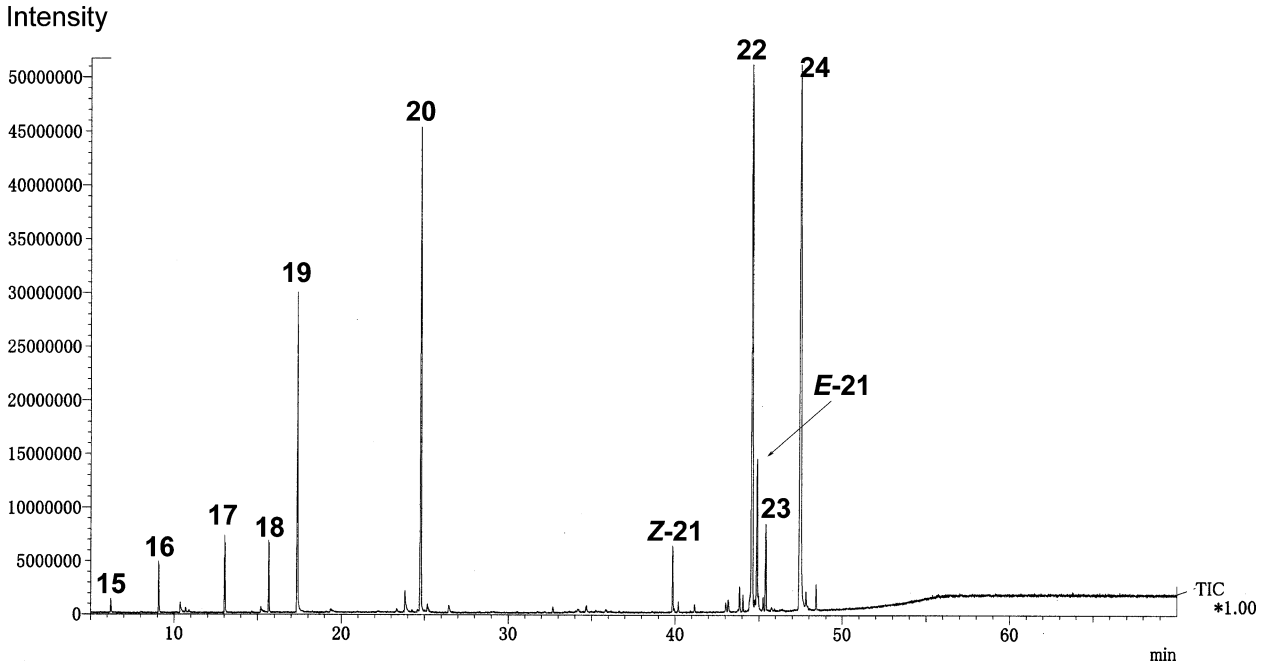

Figure 4. Pyrolysis–GC/MS trace of **2**. Pyrolysis was carried out at 500 °C for 4 s. Product names refer to those in **Table 2**; structures are given in **Figures 1** and **3** and **Scheme 1**.

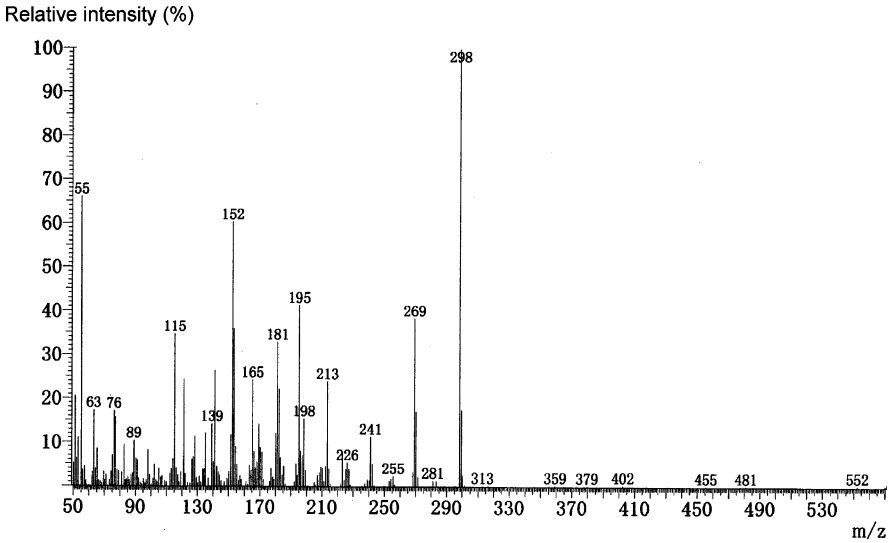

Figure 5. Mass spectrum of *E*-**21**.

to provide the corresponding pair of 4-hydroxy-3-methoxystyrene (**8**) and benzaldehyde **9** (pathway iv). Genuit et al. (*12*) also proposed that **8** and **9** are produced via a similar oxetane intermediate from β-1 subunits in softwood lignin. However, our pyrolysis conditions provided **8** in a rather smaller contribution (~1%) than expected from the contribution of **9** (7.6%). This finding and the large contribution of **10** (8%) strongly demonstrate that oxetane A is responsible for the production of **9** to a small extent and that **9** is mostly produced via pathway i + ii.

Several dimers are visible above 30 min retention time, with the largest abundance for *E*-**3**. Roughly 45% contribution (~70% contribution of identified dimers) was given by stilbenes *Z*-**3** + *E*-**3**. These isomers were identified by comparing their MS data and retention times with those of authentic **3** consisting of 97% *E*-isomer and 3% *Z*-isomer. The release of CH_2O from oxetane A by the ring cleavage (pathway v) resulted in stilbene **3** with a 1:3.6 *Z*/*E*-isomeric ratio based on the GC/MS signal area (*26*). Similar oxetane intermediate mechanisms operate in pyrolysis of β-aryl ether lignin model compounds (*27*) and in mass fragmentations of phenolic β-1 lignin model compounds (*28*). Comparison of the contribution of **3** with that of **8** shows that pathway v is favored over pathway iv in decomposition of oxetane A.

Dimeric products **13** and **14** with each ~7% relative contribution were ascribed to 4-[(1*Z*/1*E*)-2-(4-hydroxy-3-methoxyphenyl)prop-1-enyl]-2-methoxyphenol because of the 286 molecular ion [relative intensity (rel int) 100%] and the $[M - CH_3]^+$ species at *m*/*z* 271 (rel int 41% in *E*-**13**), and to 4-[2-(4-hydroxy-3-methoxyphenyl)ethyl]-2-methoxyphenol because of the molecular ion of 274 (rel int 5%) and the base ion at *m*/*z* 137 showing the presence of the $[OH(OMe)C_6H_3CH_2]^+$ species (see **Figure 3** for the mass fragmentation).

Main reactions occurring in pyrolysis of **1** are summarized as follows in order of decreasing contribution: (1) the oxetane mechanism to produce stilbene **3**, (2) the ring-side chain bond

Scheme 2. Possible Mass Fragmentation of *E*-**21**[a]

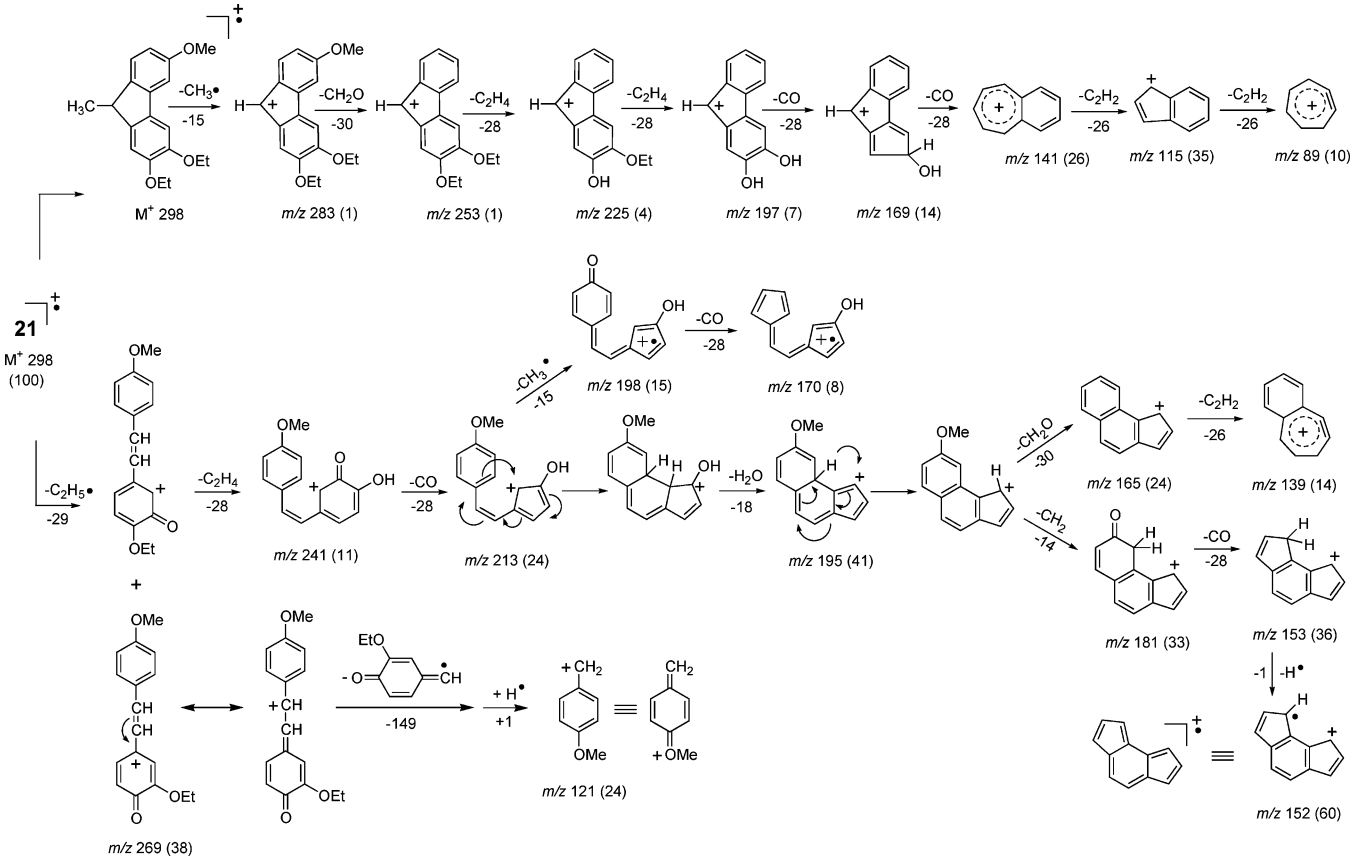

[a] Values in parentheses mean the relative intensity (percent) of the mass ion.

Scheme 3. Formation of **22**–**24** from **2**[a]

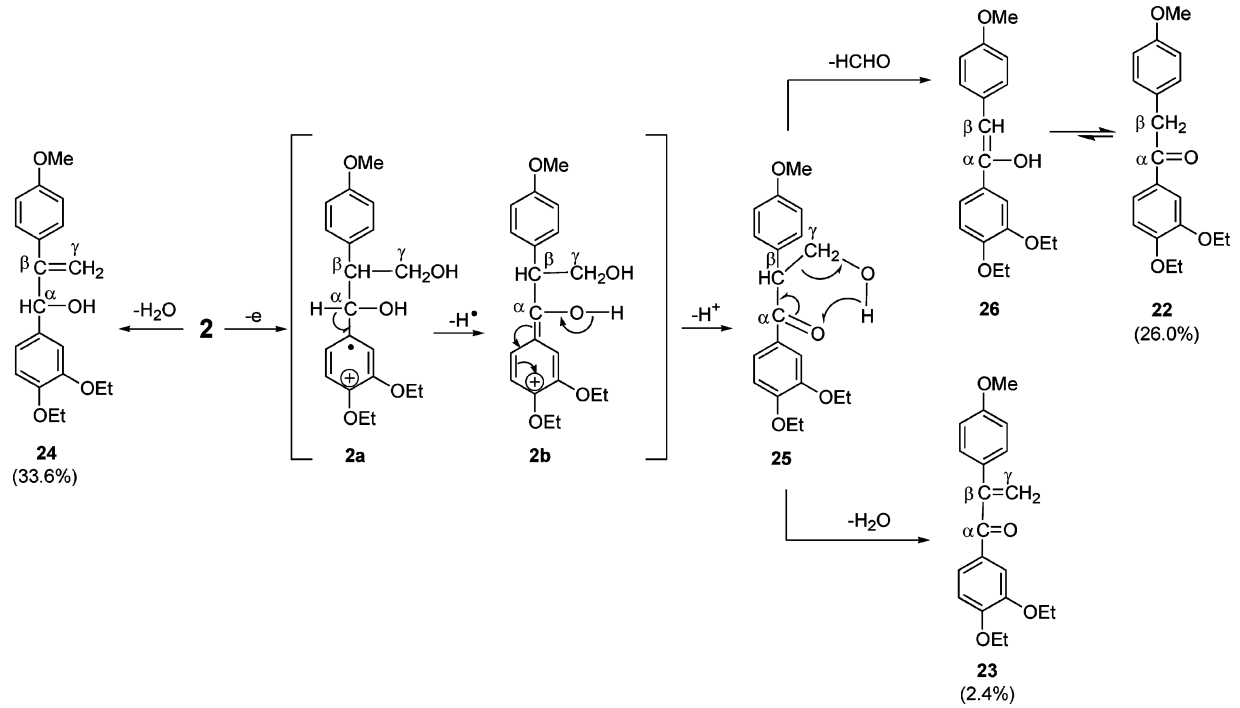

[a] Names for **22**–**24** refer to those in **Table 2**. Values in parentheses mean the relative contribution (percent) of the product.

cleavage, and (3) hydrogen transfer from the α-OH onto the Cβ atom and then the Cα−Cβ bond cleavage to produce **9** and **10**.

Pyrolysis−GC/MS of 2. Figure 4 shows the pyrolysis−GC/MS trace of **2**. **Table 2** lists identified products with the relative contributions (percent) and partial mass data.

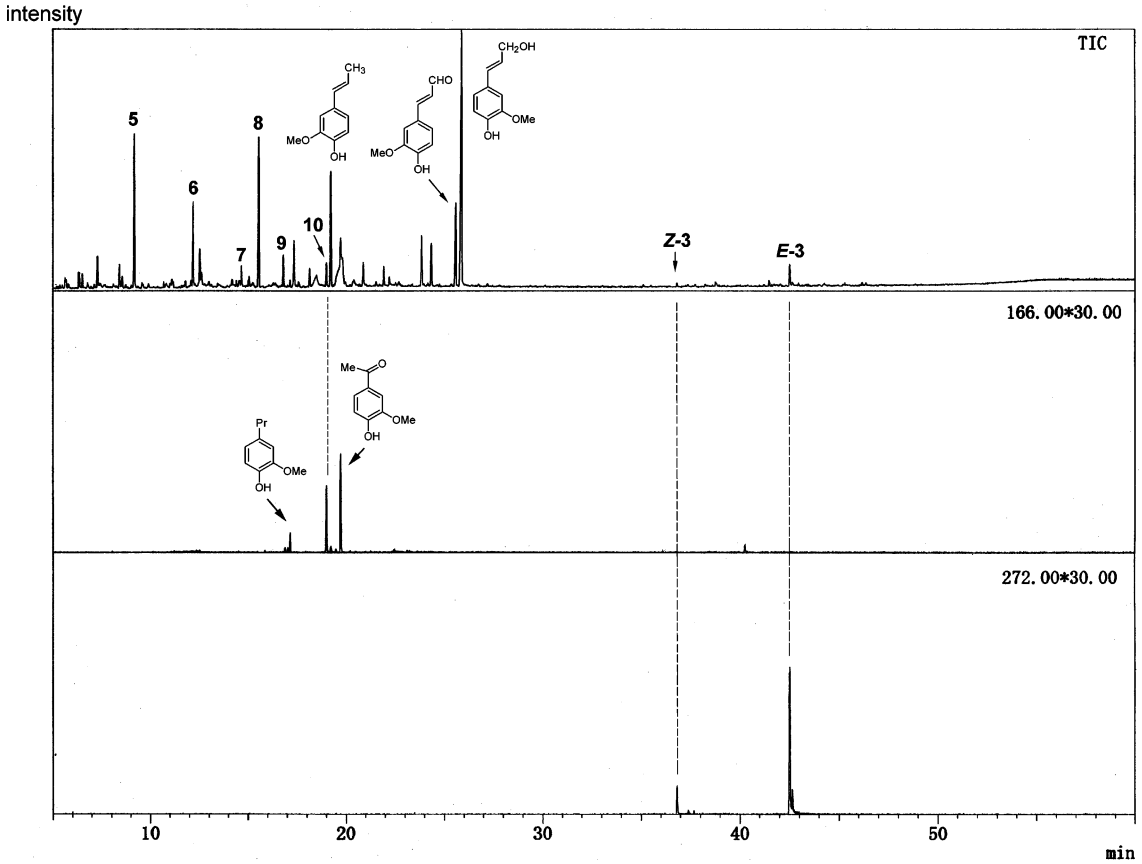

Figure 6. Pyrolysis–GC/MS trace of Japanese cedar wood (top), and the *m*/*z* 166 (middle) and *m*/*z* 272 (bottom) chromatograms. Pyrolysis was carried out at 500 °C for 4 s. Product assignments were carried out according to published data (*13*, *29*, *31*).

As in **Figure 2**, monomeric and dimeric products are revealed in **Figure 4**. Small contributions (<2%) were given by methoxybenzene (**15**, 0.2%), 4-methoxy-1-methylbenzene (**16**, 1.1%), 4-methoxystyrene (**17**, 1.8%), and 1,2-diethoxybenzene (**18**, 1.8%). The contributions of **15** and **18** produced by cleavage of the bonds between the ring and the side chain dramatically decreased compared to that of **5**, suggesting that protection of phenolic hydroxyl groups enhanced the thermal stability of β-1 subunits. Comparison of the contributions of **15** and **18** shows that ring A−Cα bond cleavage is preferred to ring B−Cβ bond cleavage in pyrolysis of **2**; this might be true for pyrolysis of **1**. The production of **16** having ring B suggests that 2-methoxy-4-methylphenol (**6**) obtained in pyrolysis of **1** also stems from moiety B.

In spite of the enhanced thermal stability, the hydrogen migration and then the Cα−Cβ bond cleavage (pathway i + ii) occurred also in pyrolysis of **2**, to produce 4-methoxyphenylethanal (**19**, 9.2%) via **28** stemming from moiety B and 3,4-diethoxybenzaldehyde (**20**, 17.7%) from moiety A. Pathway i + ii is clearly responsible for the production of **20** to a large extent, as well as for the production of **9** from **1**, because the contribution of **19** was roughly 5 times more than that of styrene **17**, the counterpart of **20** produced from oxetane B.

Dimers **21**−**24** were visible above 30 min retention time, with a large abundance for **22** and **24**. Product **21**, showing a molecular ion of 298, was assigned to 3,4-diethoxy-4′-methoxystilbene consisting of *Z*- and *E*-isomers in a 1:2.3 GC/MS signal area ratio. Although the mass spectra of stilbenes with methoxyl group(s) are generally poor in fragments revealing the molecular ion as the base ion and a low relative intensity (<10%) of the $[M - CH_3]^+$ fragment ion, the mass spectrum of **21** (**Figure 5**) revealed many informative fragment ions for structural identification, probably due to the presence of the two ethoxyl groups (compare with the MS data of **3**); the mass fragmentation is proposed in **Scheme 2**.

Also in pyrolysis of **2**, a large contribution of stilbenes was expected. Stilbene **21**, however, made an unexpectedly small contribution (*Z*- + *E*-isomers 6.2%), suggesting that oxetane B made a small contribution in pyrolysis of **2**. That is, protection of phenolic hydroxyl groups strongly reduces the contribution of the oxetane pathway to pyrolysis of β-1 subunits.

The prominent dimer **22** (26%), showing a molecular ion of 314 (rel int 3%), was assigned to 1-(3,4-diethoxyphenyl)-2-(4-methoxyphenyl)ethan-1-one because of the presence of the *m*/*z* 193 base ion, due to the $[(OEt)_2C_6H_3C{\equiv}O]^+$ species, and fragment ions due to the $[(OEt)_2C_6H_3]^+$ species at *m*/*z* 165 (rel int 32%) and the $[MeOC_6H_4CH_2]^+$ species at *m*/*z* 121 (rel int 26%) (see **Figure 3**). The *m*/*z* 137 ion (rel int 31%) may be due to the $[OEt(OH)C_6H_3]^+$ species.

Dimer **23** (2.4%) was assigned to 1-(3,4-diethoxyphenyl)-2-(4-methoxyphenyl)prop-2-en-1-one on the basis of the MS data: the molecular ion at *m*/*z* 326 (rel int 28%), the $[(OEt)_2C_6H_3C{\equiv}O]^+$ species at *m*/*z* 193 (base ion), and the $[MeOC_6H_4C{=}CH_2]^+$ species at *m*/*z* 133 (rel int 74%).

The formation of **22** and **23** may proceed via α-ketone **25** whose formation is initiated by abstraction of a single electron from ring A of **2** by thermal energy to produce a corresponding aryl cation radical **2a** (**Scheme 3**). Successively, **2a** releases a hydrogen atom at the α-position to give an α-hydroxyquinone methide cation **2b** that immediately undergoes rearrangement to produce the corresponding α-ketone **25**, with concomitant release of H^+. Ketone **25** consequently provides (1) enol **26** by migrating a hydrogen atom onto the oxygen atom of the C=O group from the γ-OH group to form a six-membered intermedi-

ate, with simultaneous elimination of the Cγ group as HCHO followed by isomerization to its tautomer **22**, and (2) **23** by β,γ-dehydration.

EI-MS analysis of the most intense **24** (33.6%) showed the molecular ion at *m*/*z* 328 (rel int <1%), the *m*/*z* 134 base ion due to the $[MeOC_6H_4CH{=}CH_2]^{+\bullet}$ species produced by a hydrogen atom shift onto the Cβ atom from the α-OH group and successive cleavage of the Cα−Cβ bond, and the *m*/*z* 195 ion (rel int 14%) due to the $[(OEt)_2C_6H_3CHOH]^+$ species. Therefore, **24** was assignable to 1-(3,4-diethoxyphenyl)-2-(4-methoxyphenyl)prop-2-en-1-ol produced by simple β,γ-dehydration of **2**.

In summary, in pyrolysis of **2** the oxetane mechanism operates as a minor pathway, and the main reactions that occurred are as follows in order of decreasing contribution: (1) β,γ-dehydration, (2) formation of α-ketone dimer, and (3) hydrogen transfer from the α-OH onto the Cβ atom and then Cα−Cβ bond cleavage.

Pyrolysis−GC of Japanese Cedar Wood. To confirm the contributions of β-1-derived products **3** and **10** to softwood lignin pyrolysates, extractive-free Japanese cedar wood and DHP were subjected to pyrolysis−GC/MS under similar conditions, the same except the column conditions, to those employed in the model experiments. **Figure 6** (top) shows the pyrolysis−GC/MS trace of Japanese cedar wood. The *m*/*z* 166 chromatogram is shown with 30-fold intensity in **Figure 6** (middle), in which three signals were displayed. Among them, a signal appearing at retention time of 19.0 min was attributed to **10**, on the basis of the fragmentation pattern and retention time and a previous result with authentic 4-hydroxy-3-methoxyphenylethanal (*29*); 2-methoxy-4-propylphenol [EI-MS *m*/*z* 166 (M^+, 20), 137 (100)] and 1-(4-hydroxy-3-methoxyphenyl)ethanone [EI-MS *m*/*z* 166 (M^+, 39), 151 (82), 60 (100), 57 (50)] were observed at 17.2 and 19.7 min, respectively. **Figure 6** (bottom) shows the *m*/*z* 272 chromatogram with 30-fold intensity. Three signals were observed. By comparing the mass fragmentation pattern and retention time of authentic **3**, the former two signals were attributed to a pair of *Z*-**3** and its *E*-form. As plausible pyrolytic sources for the *m*/*z* 272 ion, β-O-4 and β-5 subunits are also proposed (*30*), other than **3** derived from β-1 subunits. Of these, the contribution of β-5 subunits is negligible to the formation of the *m*/*z* 272 ion because dimers are observed in a very small abundance in pyrolysis of dehydrodiconiferyl alcohol, a representative β-5-type lignin model compound, at 500 °C for 4 s (*19*). Enol ether **4** is a β-O-4 subunit-derived product showing a molecular ion of 272 (*30*). However, no signals corresponding to *Z*- and *E*-**4** were revealed in the mass chromatogram for *m*/*z* 272 [**Figure 6** (bottom)].

Quantification of **3** and **10** in the cedar wood pyrolysate was carried out by pyrolysis−GC/FID (not shown). The isoeugenol yield [∼2.2% on the Klason lignin content (*31*)] and the response factors of isoeugenol, **3**, and **10** to FID, calculated by their effective carbon numbers and GC peak areas (*32*), showed that the yields of **3** and **10** were roughly 0.8% and 0.6%, respectively, on the basis of the Klason lignin content. These values appear to be smaller than expected from the abundance of softwood β-1 subunits [7% in a spruce milled wood lignin (*10*)]. This may be due to pyrolytic efficiencies.

The pyrolysis−GC/MS trace of the bulk DHP also showed *E*-**3** (not shown) but in very small abundance. This difference reflects the differences in abundance of β-1 subunits in softwood and synthetic lignins [absence in an endwise guaiacyl DHP (*33*)].

Pyrolysis directly combined with MS, pyrolysis−MS, is also introduced as a powerful lignin characterization tool with the advantages of a shorter analysis time (usually within a few seconds) and a smaller sample requirement (usually a few micrograms) than those of pyrolysis procedures with a GC column (*34*−*36*). However, since pyrolysis−MS provides a spectrum consisting of molecular and fragmentation ions derived from lignin and carbohydrates, it is more difficult to assign MS ions than for pyrolysis techniques with a GC column. This is true for pyrolysis−MS of softwood lignocellulosic materials revealing a *m*/*z* 272 ion with a considerable intensity (*30*, *34*). However, the results with pyrolysis of Japanese cedar wood clearly show that β-1 subunits make a large contribution to the intensity of the *m*/*z* 272 ion generated in pyrolysis−MS of softwood lignin.

A series of mass signals with a regular increment of 30 Da (methoxyl group substitution for H-atom), the *m*/*z* 272, 302, and 332 ions, observed in the pyrolysis−MS trace of *Aesculus turbinate* Blume milled wood lignin (*34*) may be assigned to the molecular ions of guaiacyl/guaiacyl, guaiacyl/syringyl, and syringyl/syringyl 4,4′-dihydroxy β-1 stilbenes, respectively.

LITERATURE CITED

(1) Sarkanen, K. V.; Ludwig, C. H. Definition and nomenclature. In *Lignins: Occurrence, Formation, Structure and Reactions*; Sarkanen, K. V., Ludwig, C., Eds.; John Wiley & Sons, Inc.: New York, 1971; pp 1−18.

(2) Meier, D.; Faix, O. Pyrolysis-gas chromatography-mass spectrometry. In *Methods in Lignin Chemistry*; Lin, S. Y., Dence, C. W., Eds.; Springer-Verlag: Berlin and Heidelberg, Germany, 1992; pp 177−199.

(3) Nimz, V. H. Lignin degradation by mild hydrolysis. *Holzforschung* **1966**, *20*, 105−109.

(4) Lapierre, C.; Pollet, B.; Monties, B. Heterogeneous distribution of diarylpropane structures in spruce lignins. *Phytochemistry* **1991**, *30*, 659−662.

(5) Zhang, L.; Gellerstedt, G. NMR observation of a new lignin structure, a spiro-dienone. *Chem. Commun.* **2001**, 2744−2745.

(6) Zhang, L. M.; Gellerstedt, G.; Ralph, J.; Lu, F. C. NMR studies on the occurrence of spirodienone structures in lignins. *J. Wood Chem. Technol.* **2006**, *26*, 65−79.

(7) Ede, R. M.; Ralph, J.; Torr, K. M.; Dawson, B. S. W. A 2D NMR investigation of the heterogeneity of distribution of diarylpropane structures in extracted *Pinus radiata* lignins. *Holzforschung* **1996**, *50*, 161−164.

(8) Lundquist, K. On the occurrence of β-1 structures in lignin. *J. Wood Chem. Technol.* **1987**, *7*, 179−185.

(9) Habu, N.; Matsumoto, Y.; Ishizu, A.; Nakano, J. The role of the diarylpropane structure as a minor constituent in spruce lignin. *Holzforschung* **1990**, *44*, 67−71.

(10) Lai, Y.-Z.; Sarkanen, K. V. Isolation and structural studies. In *Lignins: Occurrence, Formation, Structure and Reactions*; Sarkanen, K. V., Ludwig, C. H., Eds.; John Wiley & Sons, Inc.: New York, 1971; pp 165−240.

(11) Evans, R. J.; Milne, T. A.; Soltys, M. N. Direct mass-spectrometric studies of the pyrolysis of carbonaceous fuels III. Primary pyrolysis of lignin. *J. Anal. Appl. Pyrolysis* **1986**, *9*, 207−236.

(12) Genuit, W.; Boon, J. J.; Faix, O. Characterization of beech milled wood lignin by pyrolysis-gas chromatography-photoionization mass spectrometry. *Anal. Chem.* **1987**, *59*, 508−513.

(13) Kuroda, K.; Dimmel, D. R. Effect of pyrofoil composition on pyrolysis of lignin. *J. Anal. Appl. Pyrolysis* **2002**, *62*, 259−271.

(14) Ralph, J.; Hatfield, R. D. Pyrolysis-GC-MS characterization of forage materials. *J. Agric. Food Chem.* **1991**, *39*, 1426−1437.
(15) Ahvonen, T.; Brunow, G.; Kristersson, P.; Lundquist, K. Stereoselective syntheses of lignin model compounds of the β-O-4 and β-1. *Acta Chem. Scand.* **1983**, *B 37*, 845−849.
(16) Gierer, J.; Lenic, J.; Norén, I.; Szabo-Lin, I. Lignin chromophores. Part I. Synthesis of chromophores of the 2,4′- and 4,4′-dihydroxystilbene types. *Acta Chem. Scand.* **1974**, *B28*, 717−729.
(17) Ralph, J.; Helm, R. F.; Quideau, S. Lignin-feruloyl ester cross-links in grasses. Part 2. Model compound syntheses. *J. Chem. Soc., Perkin Trans. 1* **1992**, 2971−2980.
(18) Gierer, J.; Norén, I. Über die Reaktionen des Lignins bei der Sulfatkochung II. Modellversuche zur Spaltung von Aryl-alkylätherbindungen durch Alkali. *Acta Chem. Scand.* **1962**, *16*, 1713−1729.
(19) Kuroda, K.-I.; Nakagawa, A. Analytical pyrolysis of lignin: Products stemming from β-5 substructures. *Org. Geochem.* **2006**, *37*, 665−673.
(20) Nakagawa-izumi, A.; Kuroda, K.; Ozawa, T. Thermochemolytic behavior of β-β lignin structures in the presence of tetramethylammonium hydroxide (TMAH). *Org. Geochem.* **2004**, *35*, 763−774.
(21) Kuroda, K.; Nakagawa-izumi, A.; Dimmel, D. R. Pyrolysis of lignin in the presence of tetramethylammonium hydroxide (TMAH): Products stemming from β-5 substructures. *J. Agric. Food Chem.* **2002**, *50*, 3396−3400.
(22) Kuroda, K.; Ozawa, T.; Ueno, T. Characterization of sago palm (*Metroxylon sagu*) lignin by analytical pyrolysis. *J. Agric. Food Chem.* **2001**, *49*, 1840−1847.
(23) Mazumder, B. B.; Nakagawa-izumi, A.; Kuroda, K.; Ohtani, Y.; Sameshima, K. Evaluation of harvesting time effects on kenaf bast lignin by pyrolysis-gas chromatography. *Ind. Crops Prod.* **2005**, *21*, 17−24.
(24) Kuroda, K. Pyrolysis of arylglycol-β-propylphenyl ether lignin model in the presence of borosilicate glass fibers. 1. Pyrolysis reactions of β-ether compounds. *J. Anal. Appl. Pyrolysis* **1994**, *30*, 173−182.
(25) Kuroda, K. Analytical pyrolysis products derived from cinnamyl alcohol-end groups in lignins. *J. Anal. Appl. Pyrolysis* **2000**, *53*, 123−134.
(26) Holbrook, K. A.; Scott, R. A. Gas-phase unimolecular pyrolysis of *cis*- and *trans*-2,3-dimethoxyoxetane. *J. Chem. Soc., Faraday Trans. I.* **1974**, *70*, 43−50.
(27) Brežný, R.; Mihálov, V.; Kováčik, V. Low temperature thermolysis of lignins I. Reactions of β-O-4 model compounds. *Holzforschung* **1983**, *37*, 199−204.
(28) Kováčik, V.; Mihálov, V.; Brežný, R. Mass spectrometry of lignin model substances. III. Structure determination of β-linked dimers by mass spectrometry. *Cellul. Chem. Technol.* **1980**, *14*, 233−241.
(29) Kuroda, K.; Mun, S.-P.; Sakai, K. Analytical pyrolysis of alcohol bisulfite lignin. *J. Anal. Appl. Pyrolysis* **1995**, *31*, 239−247.
(30) van der Hage, E. R. E.; Mulder, M. M.; Boon, J. J. Structural characterization of lignin polymers by temperature-resolved in-source pyrolysis-mass spectrometry and Curie-point pyrolysis-gas chromatography/mass spectrometry. *J. Anal. Appl. Pyrolysis* **1993**, *25*, 149−183.
(31) Kuroda, K.; Yamaguchi, A.; Sakai, K. Analysis of sugi (Japanese cedar) wood and its lignin preparations by pyrolysis-gas chromatography. *Mokuzai Gakkaishi* **1994**, *40*, 987−995.
(32) Jorgensen, A. D.; Picel, K. C.; Stamoudis, V. C. Prediction of gas chromatography flame ionization detector response factors from molecular structures. *Anal. Chem.* **1990**, *62*, 683−689.
(33) Landucci, L. L. Reaction of *p*-hydroxycinnamyl alcohols with transition metal salts. 1. Oligolignols and polylignols (DHPs) from coniferyl alcohol. *J. Wood Chem. Technol.* **1995**, *15*, 349−368.
(34) Izumi, A.; Kuroda, K. Pyrolysis-mass spectrometry analysis of dehydrogenation polymers with various guaiacyl/syringyl ratios. *Rapid Commun. Mass Spectrom.* **1997**, *11*, 1405−1411.
(35) Vermerris, W.; Boon, J. J. Tissue-specific patterns of lignification are disturbed in the brown midrib2 mutant of maize (*Zea mays* L.). *J. Agric. Food Chem.* **2001**, *49*, 721−728.
(36) MacKay, J.; Dimmel, D. R.; Boon, J. J. Pyrolysis mass spectral characterization of wood from CAD-deficient pine. *J. Wood Chem. Technol.* **2001**, *21*, 19−29.

Received for review October 1, 2006. Revised manuscript received January 18, 2007. Accepted January 22, 2007.

JF0628126